Available online at www.sciencedirect.com
SCIENCE DIRECT
Journal of Geochemical Exploration 89 (2006) 231–234
JOURNAL OF GEOCHEMICAL EXPLORATION
www.elsevier.com/locate/jgeoexp

Structural controls on fluid flow and related mineralization in the Xiangshan uranium deposit, Southern China

Ge Lin [a,*], Ye Zhou [a], Xiangrong Wei [a], Chongbin Zhao [b]

[a] *Key Laboratory of Marginal Sea Geology, Guangzhou Institute of Geochemistry, Chinese Academy of Sciences, Guangzhou, 510640, PR China*
[b] *CSIRO Division of Exploration and Mining, P. O. Box 1130, Bentley, WA 6102, Australia*

Received 9 August 2005; accepted 4 November 2005
Available online 15 March 2006

Abstract

The Xiangshan uranium deposit of Southern China is a Mesozoic volcanic uranium deposit where mineralization is closely associated with regional rock deformation and fluid flow. To better understand the genesis of this deposit, we have carried out coupled deformation and fluid flow modeling to explore the relationship between mineralizing fluid flow and structural deformation processes. The numerical modeling results demonstrate that fluid transport and focusing are predominantly controlled by deposit scale structures and associated rock deformation.

Keywords: Structural-fluid modelling; Mineralization; Xiangshan uranium deposit; China

1. Introduction

Rock deformation and fluid flow are important processes that control epigenetic mineralization under a wide range of tectonic settings. Because of the importance of structural control on mineralization, the deformation history and structural characteristics of a mineralization district need to be considered in an exploration model. Since fluid is a main carrier to transport metals, the ore-bearing fluid flow in a hydrothermal system, in close interaction with rock deformation, plays an important role in ore body formation (Hobbs et al., 2000; Cox et al., 2001).

Recent development of coupled deformation and fluid flow modelling and its application to investigations of the formation of ore deposits (e.g. Ord and Oliver, 1997) have expanded our capability to consider the complexity of feedback interactions between rock deformation and mineralizing fluid flow. Recent numerical simulation results (Zhao et al., 2002; Lin et al., 2003) have indicated that ore-bearing fluid flow velocity, pathways and temperatures have different patterns in different structural environments and, therefore, the dissolution and deposition patterns of ore minerals have different characteristics. This critically controls the transportation and enrichment of ore-forming minerals and the formation of ore bodies.

Taking the Xiangshan uranium deposit in Jiangxi Province, Southern China as an example, a finite difference code, FLAC (Itasca, 2000), has been used to investigate the control of the geological structures in the Xiangshan Basin on fluid flow pattern and related mineralization in this paper. In the numerical simulation, rock materials and geometries of geological structures

* Corresponding author. Tel.: +86 20 85290763; fax: +86 20 85290130.
E-mail address: gelin@gig.ac.cn (G. Lin).

0375-6742/$ - see front matter © 2006 Elsevier B.V. All rights reserved.
doi:10.1016/j.gexplo.2005.11.051

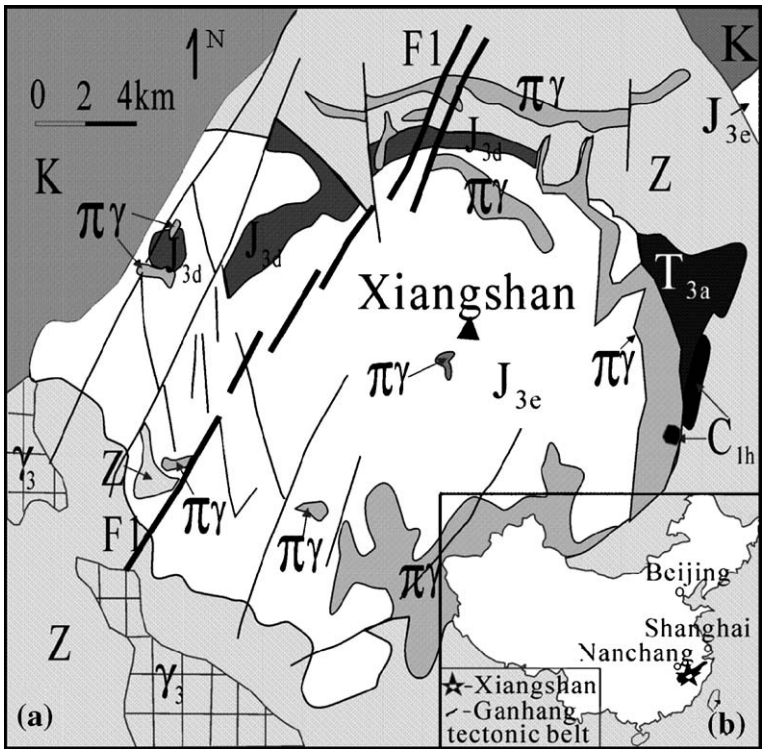

Fig. 1. (a) The structural outlines of the Xiangshan Basin: K—Upper Cretaceous gravel–sandstone; J_3e—Upper Jurassic porphyroclastic lava; J_3d—Upper Jurassic rhyolite–dacite; T_3a—Upper Tricassic gravel–sandstone; C_1h—Lower Carboniferous shale–sandstone; Z—Late Proterozoic metamorphic rockes; πγ—Upper Jurassic granite–porphyry; γ_3—Caledonian granite. (b) The location of the Xiangshan Basin in the sketch map of China.

are modelled by 2D elements. Interaction of rock deformation with porous fluid flow is simulated using the Mohr–Coulomb elastic–plastic constitutive laws in combination with Darcy's law for fluid flow (see Ord and Oliver, 1997).

2. Numerical simulation of the Xiangshan U-deposit, Southern China

The Xiangshan Basin in Jiangxi Province is located in the south-west part of Ganhang volcanic belt (Fig. 1). A Mesozoic volcanic uranium deposit, the Xiangshan deposit, was found in this basin (Li et al., 2002). The mineralization process of the Xiangshan uranium deposit involved the following three stages: (1) a compression stage, (2) an extension stage, and (3) a compression stage. The current model only investigates the structural deformation and fluid flow pattern in the first stage. As the consequence of the first compression event, a series of folds and thrust faults developed. Other secondary minor structures in the folded structure include mainly brittle fractures and brecciation zones.

The initial geometry of the 2D coupled deformation and fluid flow model is based on the structures of the P51 exploration profile through the deposit (Fig. 2). The section consists of five stratigraphic units. Geometrical inversion modeling, which is based on cross-section balancing principles, has been conducted to recover some shortening deformation along the profile. Since the main purpose of the current numerical model is to simulate fluid flow patterns during regional folding rather than fold initiation and development, we have run the numerical model with some pre-existing fold structures and faults in the district. The numerical models are initialized with a lithostatic pore-fluid pressure gradient and are subjected to horizontal shortening to simulate further folding and the associated fluid flow. The material properties of the numerical model have been chosen according to rock types and data in the literature.

Fig. 2a to e shows the numerical results and Fig. 2f illustrates the geological structures of the P51 exploration profile. A zoom-in region (see Fig. 2a) is used to show the detailed deformation and fluid flow patterns at 24% bulk shortening. During the simulated shortening

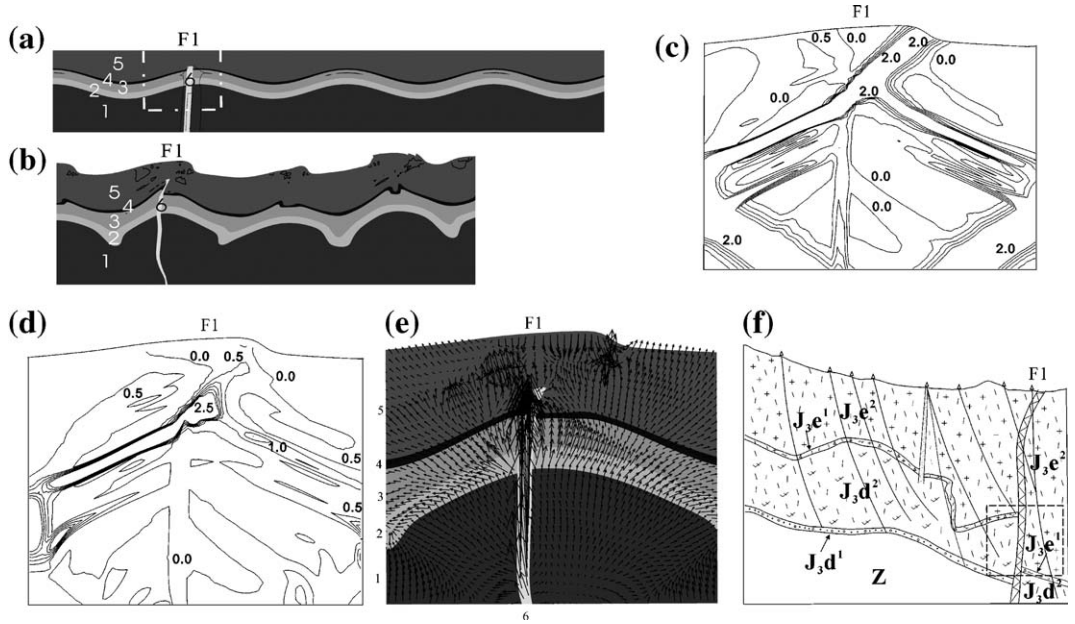

Fig. 2. Numerical results and the geological structures of the P51 profile: (a) the model geometry and tensile stress at about 5% bulk shortening; (b) the deformed geometry and tensile stress at about 24% bulk shortening; (c) shear strain distribution in the outlined zoom-in region of (a), min=0, max=2.0*e*− 4; (d) volumetric strain (dilation) distribution in the zoom-in region of (a), min=0, max=2.5*e*− 4; (e) distributions of instantaneous Darcy fluid flow velocities in the zoom-in region of (a), max=5.125*e*− 9 m/s; (f) the geological structures of the P51 exploration profile and the dash line square outlines a zoom-in region around the F_1 fault. Legends are: 1—Z: metamorphic rocks, 2—J_3d^1: sandstone; 3—J_3d^2: rhyolite–dacite; 4—J_3e^1: tuff; 5—J_3e^2: porphyroclastic lava; 6—F_1: fault.

process, tension regions occur locally in the section under the overall compressive setting. The resulting tension region gradually migrates upwards along with the increase of compressive deformation (see Fig. 2a and b). Fig. 2c and d shows the deformed geometry, shear strain and volumetric strain distributions in the zoom-in region as outlined in Fig. 2a. Note that the contour values of shear strain and volumetric strain are multiplied by 10,000 in Fig. 2c and d. It can be observed, from Fig. 2b, that the folds in the model continue to grow when the bulk shortening is increased from its initial value of 5% to its final value of 24%. The high shear strains (Fig. 2c) are mainly localized on the hanging wall and ramp positions of thrust faults and fold limbs. The fold trains in the rock sequences below the unconformity become tighter with steeper fold limbs, and the folds in the rocks above the unconformity still exhibit broad fold geometry with gently dipping limbs. The distribution of shear strain and volumetric strain (Fig. 2d) in the folded sequences is inhomogeneous. There is shear strain localization along bedding planes, especially at fold limbs, indicating intensive layer-parallel shearing during folding. This is consistent with the field observation that severe deformation (e.g. fracturing, brecciation and foliation) occurs along bedding, and some small faults develop along bedding. Obviously, there is widespread volume increase or dilation in the numerical model, reflecting the consequence of the buckling process. High dilation that is predominantly localized at fold hinges is a direct result of differential buckling between different units. High dilation that is caused by shear deformation can be also seen along bedding at fold limbs.

Fig. 2e shows fluid flow patterns within the zoom-in region of the numerical model. Generally, the fluid flow in a folded system is controlled by the deformation characteristics of the folded system. The model suggests that fluids flow along higher permeability layers to the fold hinges and core locations. Due to the effect of inhomogeneous rock deformation in high strain regions, the permeability of the layer will increase, so that the enhancement of permeability might take place at fold hinges (or fold core regions in the folding system) and limbs. This may create a favorable environment for mineralizing fluids to flow through different layers. As a result, the fluids can flow across low permeability units for a long distance and focus into fold hinge/core areas at greater velocities (see Fig. 2e), resulting in favorable mineralization sites. The results in Fig. 2e also show that faults are the major flow channels of ore-forming fluids. In addition, it is recognized that low-stress regions surrounded by high-stress ones are the favorable locations for fluid

focusing, implying that low-stress regions in the vicinity of a fault are favorable locations for fluid flow focusing.

3. Discussions and conclusions

The current numerical model not only reproduced the structural deformation of various layers in the district of the Xiangshan uranium deposit during the first compressive event, but also simulated the connection between upthrusting and the bedding collapse structures of the basin. In correlation with the field observations, the numerical simulation results are reasonably consistent with the structural features of the P51 profile in the west part of the Xiangshan uranium deposit (see the outlined region of Fig. 2f).

The numerical results also demonstrate that fluid flow is mainly controlled by the major geological structures (thrust faults and folds) of the Xiangshan Basin. For example, faults are the major flow channels for ore-forming fluids in this particular basin. In addition, the low-stress regions surrounded by high-stress ones are the favorable locations for fluid focusing, implying that low-stress regions in the vicinity of a fault are favorable locations for fluid flow focusing and the related mineralization.

Acknowledgements

This study is financially supported by the Chinese Ministry of Science and Technology (No. 2002CB412601) and Guangzhou Institute of Geochemistry, CAS (GIGCX-03-02 and 030513).

References

Cox, S.F., Knackstedt, M.A., Braun, J., 2001. Principles of structural control on permeability and fluid flow in hydrothermal systems. Reviews in Economic Geology 14, 1–24.

Hobbs, B.E., Zhang, Y., Ord, A., Zhao, C., 2000. Application of coupled deformation, fluid flow, thermal and chemical modelling to predictive mineral exploration. Journal of Geochemical Exploration 69–70, 505–509.

Itasca, 2000. FLAC: Fast Lagrangian Analysis of Continua, User Manual, Version 4.0. Itasca Consulting Group, Inc., Minneapolis.

Li, J.W., Zhou, M.F., Li, X.F., Fu, Z.R., Li, Z.J., 2002. Structural control on uranium mineralization in South China: implications for fluid flow in continental strike-slip faults. Science in China Series D 45, 851–864.

Lin, G., Zhao, C., Wang, Y.J., Hobbs, B.E., Gong, J.W., 2003. The numerical modelling of the reactive fluids mixing and the dynamic equilibrium of mineralization. Acta Petrologica Sinica 19 (2), 275–282 (in Chinese with English abstract).

Ord, A., Oliver, N.H.S., 1997. Mechanical controls on fluid flow during regional metamorphism: some numerical models. Journal of Metamorphic Geology 15, 345–359.

Zhao, C., Hobbs, B.E., Mühlhaus, H.B., Ord, A., Lin, G., 2002. Computer simulations of coupled problems in geological and geochemical systems. Computer Methods in Applied Mechanics and Engineering 191, 3137–3152.